Journal of Geodetic Science
DOI: 10.2478/jogs-2013-0010 •

Analyzing the tidal frequency content using Karhunen-Loeve Expansion technique

Research Article

M. Yousefi*, M. Mashhadi Hossainali

Abstract:
The Karhunen-Loeve Expansion (KLE) technique has been recently applied by geophysicists for analyzing the temporal variations of dynamic systems such as the ocean-atmosphere interface, crustal deformation and fault systems. The application of this method to tidal data can provide a direct insight into the efficiency and reliability of this method in reconstructing a periodic signal. The comparison of the obtained results to those proposed by the least squares harmonic estimation (LSHE) as a newly developed method which is widely used in geodetic community for analyzing the GPS time series can be of significant interest for both geodesists and geophysicists. This paper applies the KLE method to the tidal time series of the Workington station in United Kingdom and compares the given results to those suggested by the LSHE method. The detection of the majority of the expected long period constituents and the larger number of the detected low frequency components by KLE as compared to the least squares harmonic estimation emphasizes on the efficiency and the predominance of this method to the LSHE technique.

Keywords:
Karhunen-Loeve Expansion technique • spectral analysis • tidal constituents

Received 15-01-2013; accepted 10-03-2013

1. Introduction

Tide which forms a considerable part of sea level variations but are a system with a well-known mechanism. The response of this system is typically considered to be the result of the combination of harmonic terms with known frequencies. The main tidal constituents are generated from different relative motions of the Earth with respect to the Moon, Sun and consequently, the corresponding mutual gravitational forces. Earth rotation and revolution, moon rotation, motion of the lunar perigee, lunar node and solar precession are the main causing forces of the tide.

The renowned procedures for identifying and analysis of the known frequency contents of tide can be generally classified into Non-Harmonic and Harmonic methods. The Non-Harmonic method was initiated by Sir John Lubbock (1831). This method is based on the direct computation of the tidal potential using astronomical ephemerides and Kepler-Newtonian mechanics (Longman 1959, Munk and Cartwright 1966, Harrison 1971, Merriam 1992). In Harmonic Analysis (which was initially developed by Lord Kelvin and Sir George Darwin in the 1860s), sea level changes for a point at time t $(\zeta(t))$ can be formulated in terms of the sum of cosine terms whose frequencies, amplitudes and phases are C_k, ω_k and θ_k respectively; i.e., $\zeta(t) = \sum_k C_k \cos(\omega_k + \theta_k)$. The frequency content in the tidal observations (ω_k) can be determined through the application of various harmonic decomposition and spectral analysis techniques. Among the existing methods, Fourier Transform, wavelet analysis and recently the Least-Squares Harmonic Estimation (LSHE) are usually suggested and used (Doodson 1921, Tamura 1987, Cartwright and Tayler 1971, Hartmann and Wenzel, 1995, Roosbeek 1995, Jay and Flinchem 1997, Kudryavtsev 2004, Foreman and Cherniawsky 2009, Amiri-Simkooei 2007, Mousavian and M. Hossainali 2012). For the purpose of tidal analysis and tidal prediction, computation of the amplitudes (C_k) and phases (θ_k) of the dominant frequencies is usually sufficient. The least-squares adjustment of observational errors is used for this purpose.

*E-mail: yousefi67@yahoo.com

Tide, with the total number of 26753 known frequencies (Kudryavtsev 2004) is a dynamic system with well established frequency content. Some of the known constituents in this phenomenon are given in Table 1. Therefore, further analysis of this system in the frequency domain does not seem to be an interesting subject, at least from an engineering point of view. Nevertheless, the system provides a valuable measure for the analysis and comparison of proposed component decomposition and spectral analysis techniques. The idea looks more interesting when the application of such methods for analyzing the GPS coordinate time series is taken into account. Therefore, the employment of new techniques to well-known periodic phenomena such as the tide can provide a reasonable insight into their efficiency in practice. In this paper, the Karhunen-Loeve Expansion and Least-Squares Harmonic Estimation are applied to the tidal time series for this purpose.

Similar to the method of Empirical Orthogonal Function (EOF) analysis developed by Preisendorfer (1988), the method of Karhunen-Loeve Expansion (KLE) decomposes a dynamic system into its orthonormal subspaces. This technique has been applied to the analysis of many nonlinear systems such as ocean-atmosphere interface (e.g. El Niño-Southern Oscillation phenomena), meteorology, crustal deformation and fault systems (Preisendorfer 1988, Savage 1988, Penland 1993, Rundle et al. 2000, Tiampo et al. 2004). The great success of the application of this method in previous fields of research, especially ocean-atmosphere interface analysis, gives rise to the idea of its application to the tide as a nonlinear system from its principal components aspect. In this paper, the efficiency of the KLE method in the extraction of the frequency content of tidal variations as a phenomenon with a well-known mechanism is evaluated and the obtained results are compared with the LSHE method, recently carried out by Mousavian and Hossainali.

2. Material and Methodology

Understanding the pattern evolution in nonlinear systems helps for characterizing the physics which controls the underlying dynamics of a physical phenomenon. In this context, the Karhunen-Loeve Expansion can be applied to provide a complete and unique temporal pattern basis set for such systems. Here the tide, as a considerable part of the sea level variations, is investigated as a nonlinear system with a well-known physical mechanism. In the KLE technique, the correlation matrix of the input stochastic or deterministic variables is decomposed to its orthonormal subspaces known as "KLE modes". The projection of the original input data to these eigenmodes, also known as Principal Components (PC), can demonstrate the contribution of each mode to the variations of the system. A Discrete Fourier Transform accompanied by a statistical hypothesis test can be applied for investigating the frequency content of each principal component. In other words, to extract the intrinsic features of the corresponding power spectra, one may have to investigate each power spectrum against an appropriate null hypothesis. In this paper, an autoregressive process at 95% confidence level is used as the background noise model for the ex-

Table 1. Dominant tidal Harmonics (Wahr 1995, House 1995).

No.	Period (hours)	Darwin symbol
Long-period tides		
1	163154.3167	N
2	8766.15265	Sa
3	4383.0763	Ssa
4	763.4874	Msm
5	661.3111	Mm
6	354.36706	Msf
7	327.859	Mf
8	219.1904	Mtm
Diurnal tides		
9	28.0062	$2Q_1$
10	27.8483	σ_1
11	26.8683	Q_1
12	26.7230	ρ_1
13	25.8193	O_1
14	24.8412	M_1
15	24.1321	π_1
16	24.06588	P_1
17	24	S_1
18	23.9344	K_1
19	23.8044	ϕ_1
20	23.09848	J_1
21	22.3060	OO_1
Semidiurnal tides		
22	13.1272	ε_2
23	12.905	$2N_2$
24	12.871	μ_2
25	12.658	N_2
26	12.626	υ_2
27	12.4206	M_2
28	12.221	λ_2
29	12.191	L_2
30	12.016	T_2
31	12	S_2
32	11.983	R_2
33	11.967	K_2
34	11.606	$2SM_2$
Short-period tides		
35	8.3863	$2MK_3$
36	8.2863	M_3
37	8.1771	MK_3
38	6.26917	MN_4
39	6.10333	MS_4
40	6.02103	M_4
41	6	S_4
42	4.1404	M_6
43	4	S_6
44	3.10515	M_8

traction of the dominant constituents in tide.

In univariate KLE analysis of the tidal system, the required input is the detrended sea level measurements of a tide gauge. To be more specific, the hourly sea level measurements of each day collaborate on forming the columns of an input matrix, say T. As the result, when the tidal data of one year length were to be analyzed, matrix T would have the dimension of 24×365. The covariance matrix of the time series (S) is then constructed by the product: $\mathsf{T}^T\mathsf{T}$. When this real valued, symmetric matrix is normalized by the variance vector σ, i.e., $S_{ij} / \left(\sigma_i \sigma_j\right)$, the resulting correlation matrix C is derived:

$$\mathsf{C} = \begin{bmatrix} \frac{S_{11}}{\sigma_1\sigma_1} & \frac{S_{12}}{\sigma_1\sigma_2} & \cdots & \frac{S_{1p}}{\sigma_1\sigma_p} \\ \frac{S_{21}}{\sigma_2\sigma_1} & \frac{S_{22}}{\sigma_2\sigma_2} & \cdots & \frac{S_{2p}}{\sigma_2\sigma_p} \\ . & . & & . \\ . & . & \cdots & . \\ . & . & & . \\ \frac{S_{p1}}{\sigma_p\sigma_1} & \frac{S_{p2}}{\sigma_p\sigma_2} & \cdots & \frac{S_{pp}}{\sigma_p\sigma_p} \end{bmatrix} \tag{1}$$

where the variances, σ_j, are given by the following equation:

$$\sigma_j = \sqrt{\frac{1}{p}\sum_{k=1}^{p}\left(T_{kj}\right)^2} \tag{2}$$

The covariance matrix C is a $p \times p$ positive-valued matrix which can be decomposed as:

$$\mathsf{C} = \mathsf{E}\Lambda\mathsf{E}^T \tag{3}$$

where E and Λ are the eigenvector with orthonormal columns and the diagonal matrix of the eigenvalues, respectively. The matrix Λ has k ($p \geqslant k$) nonzero diagonal eigenvalues $\{\lambda_k\}$. For real geodetic or geophysical data, the rank of matrix C is usually full ($k = p$) (Dong 2006). This can be easily verified through the number of nonzero eigenvalues. The corresponding eigenvalues and eigenvectors are derived in two steps. First, Householder reduction is applied as a tireduction technique to reduce the correlation matrix to a symmetric tridiagonal one (Press et al. 1992). Then a QL algorithm is employed to find the eigenvalues, λ_j, and eigenvectors, $\mathbf{e}_j$, of the tridiagonal matrix computed in the previous step (Press et al. 1992). Computed eigenvectors are also called KLE modes.

The projection of the vectorized form of initial data series onto the eigenvectors of the data correlation matrix leads to the principal component associated with each particular mode.

The next step is the spectral analysis of the principal components computed in the previous step. For this purpose, firstly the Discrete Fourier Transform is used for constructing the Fourier power spectrum of each principal component. A statistical significance test is then applied to the derived Fourier spectrum in order to extract the intrinsic features inherent in the power spectra. This is done in support of a null hypothesis for the background noise model at 95% of confidence level. For many geophysical phenomena the red noise model, i.e. the first order autoregressive (AR) process is considered to be an appropriate background noise model (Mann and Lees 1996, Ghil et al. 2002). According to Allen and Smith (1996), the presence of periodic effects should be explicitly taken into account in the AR parameter estimation process. The identification of periodicities and their physical causes seems to be hard for most geophysical systems. On the other hand, this by itself is the main aim in the spectral analysis of a time series. To solve this problem, well-established frequencies are normally used for detrending the input data. The Principal lunar semidiurnal constituent M_2, Principal solar semi diurnal constituent S_2, Solar annual constituent Sa, Solar semiannual constituent Ssa, Lunisolar semi diurnal constituent K_2, Larger lunar elliptic semi diurnal constituent N_2, Lunisolar diurnal constituent K_1, and Lunar diurnal constituent O_1 are the periodic components which have been used to fit an autoregressive process and for estimating the corresponding parameters. A univariate lag-1 autoregressive process can be written as:

$$x_0 = 0, \quad x_n = \alpha x_{n-1} + Z_n, \quad n = 1, \ldots, N \tag{4}$$

where x_n is the discrete time series with the initial value of x_0, N is the number of points in the time series, $\{Z_n\}$ are Gaussian random variables, and α is the autoregressive coefficient which can be computed from the following equation (Brockwell and Davis 1991):

$$\alpha = \frac{\frac{1}{N-1}\sum_{i=1}^{N-1}(x_i - \bar{x})(x_{i+1} - \bar{x})}{\frac{1}{N}\sum_{i=1}^{N}(x_i - \bar{x})^2} \tag{5}$$

where $\bar{x}$ is the mathematical expectation of the time series. Torrence and Compo (1998) showed that the probability density function of the Fourier power spectrum of an autoregressive process with the coefficient α, defined by Eq. (5), is as follows:

$$\frac{\tilde{\sigma}^2(1-\alpha^2)}{2N\left(1+\alpha^2-2\alpha\cos\frac{2\pi n}{N}\right)}\chi^2_{2,0.95} \tag{6}$$

where $\tilde{\sigma}^2$ is the variance of time series, and χ^2_2 is the chi-squared distribution with two degrees of freedom. Equation (6) provides a measure for identifying the constituents which significantly contribute in re-constructing the original time series. For this purpose, a peak in the Fourier spectrum is taken as a true signal when it lies above the background noise whose probability density function is given by this equation. The probability that is assigned to the detected frequencies here is 0.95.

3. Numerical Results

The United Kingdom's Tide Gauge Network has provided the required inputs for this study. The tidal time series from station Workington has been used for this purpose. This is because least squares harmonic estimation has been already applied for analyzing the frequency content at the position of

Table 2. First Principal Component tidal constituents.

No.	Frequency (hour^{-1})	symbol	No.	Frequency (hour^{-1})	symbol
1	0.0001141	*Sa*	21	0.0820776	NKM_2
2	0.0002283	*Ssa*	22	0.0831050	$2SK_2$
3	0.0005707		23	0.0833333	S_2
4	0.0012557		24	0.0835616	K_2
5	0.0014840	*Mm*	25	0.0840182	
6	0.0030821	*Mf*	26	0.0842465	
7	0.0372146	Q_1	27	0.0848173	MSN_2
8	0.0386986	O_1	28	0.0861872	$2SM_2$
9	0.0415525	P_1	29	0.0864155	SKM_2
10	0.0417808	K_1	30	0.1207762	M_3
11	0.0759132	OQ_2	31	0.1579908	N_4
12	0.0761415	$\varepsilon 2$	32	0.1594748	MN_4
13	0.0773972	$2N_2$	33	0.1610730	M_4
14	0.0777397		34	0.1623287	SN_4
15	0.0779680		35	0.1625570	NK_4
16	0.0786529		36	0.1638127	MS_4
17	0.0789954	N_2	37	0.1640410	MK_4
18	0.0792237	$\upsilon 2$	38	0.2415525	M_6
19	0.0804794	M_2	39	0.2444063	$2MS_6$
20	0.0817351				

this tidal station. The corresponding time series of this station is available at https://www.bodc.ac.uk/data/online_edelivery/ntslf/processed/. One year of equi-spaced hourly tidal records of this station has been incorporated in the input matrix $\mathbf{T}$.

At first, the correlation matrix (1) is computed from the input matrix $\mathbf{T}$. Using the QL algorithm the reduced tridiagonal form of the correlation matrix is then transformed to the corresponding eigenspace. This process leads to the eigenmodes of interest. The constructed eigenmodes establish an empirical orthonormal basis which can be used for the decomposition and further analysis of the original data. Therefore, the tidal time series is projected onto the principal direction defined by the empirical basis above. Applying Fourier transform to the projected time series results in the corresponding power spectra which are further used for detecting the tidal constituents. Fitting an autoregressive process to each power spectrum provides a statistical measure for selecting the dominant frequencies. Figure 1 illustrates the corresponding results for the first eingenmode of this research. Accepted frequencies are listed in Table 2.

The contribution of the first eigenmode in the total sea level variations at this station is 84.49 precent of the total sea level variations inherent in the adopted time series. Therefore, the first eigenmode is expected to contain most of the dominant frequencies in a tidal time series. This can be seen in Fig. 1. In this figure, the first three prominent amplitudes belong to the principal lunar semidiurnal component (M_2), principal solar semidiurnal constituent (S_2), and larger lunar elliptic semidiurnal component (N_2) respectively.

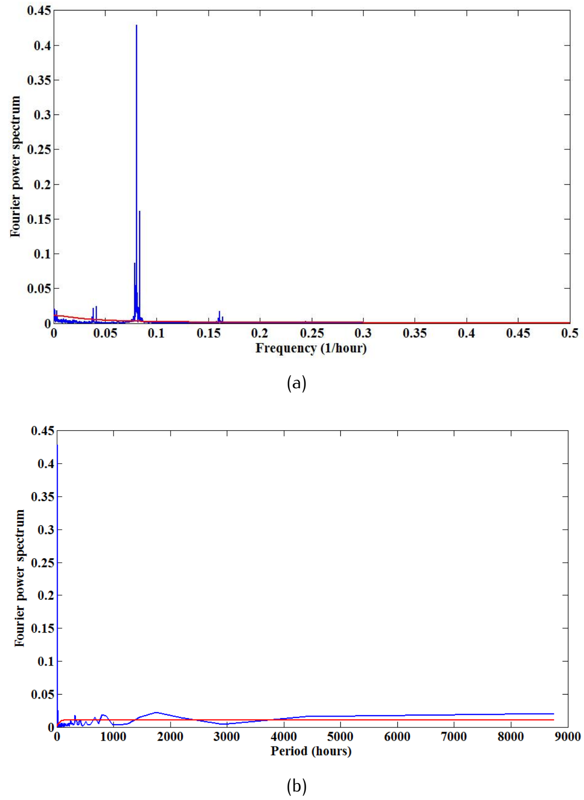

Figure 1. Fourier power spectrum of first PC normalized by $N/2\sigma^2$ (blue) with respect to frequency (top) and period (bottom) as well as the background noise model at 99% confidence level (red).

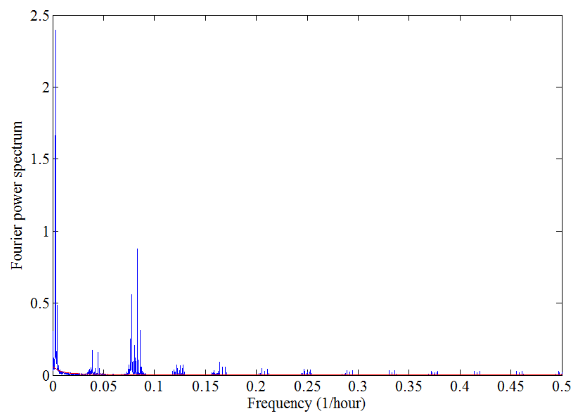

Figure 2. Fourier power spectrum of second PC normalized by $N/2\sigma^2$.

The Fourier power spectrum of the second principal component and the correspondingly detected frequencies are illustrated and reported in Fig. 2 and Table 3, respectively. The Lunisolar synodic

Table 3. Second Principal Component tidal constituents.

No.	Freqency (hour^{-1})	symbol	No.	Freqency (hour^{-1})	symbol
1	0.0002283	Ssa	39	0.1206621	M_3
2	0.0013698	Msm	40	0.1221461	MS_3
3	0.0028538	Msf	41	0.1250000	S_3
4	0.0041095	$S\upsilon_2$	42	0.1278538	
5	0.0043378	SN	43	0.1293378	
6	0.0055936	$2SM$	44	0.1567351	
7	0.0058219	$MSqm$	45	0.1582191	$3MS_4$
8	0.0343607	α_1	46	0.1623287	SN_4
9	0.0345890		47	0.1638127	MS_4
10	0.0360730		48	0.1666666	S_4
11	0.0373287	ρ_1	49	0.1695205	$3SM_4$
12	0.0384703		50	0.1710045	
13	0.0388127	MS_1	51	0.2027397	$2MK_5$
14	0.0390410	τ_1	52	0.2039954	
15	0.0400684	β_1	53	0.2054794	MSP_5
16	0.0416666	S_1	54	0.2083333	
17	0.0445205		55	0.2111872	
18	0.0460045		56	0.2471461	$2SM_6$
19	0.0731735		57	0.2500000	S_6
20	0.0746575	$2NS_2$	58	0.2528538	
21	0.0761415	ε_2	59	0.2873287	
22	0.0777397		60	0.2888127	
23	0.0787671	SNK_2	61	0.2916666	
24	0.0792237	υ_2	62	0.2945205	
25	0.0802511	γ_2	63	0.3304794	$3SM_8$
26	0.0807077	MKS_2	64	0.3333333	S_8
27	0.0818493	$\lambda 2$	65	0.3361872	
28	0.0820776	NKM_2	66	0.3721461	NK_1
29	0.0833333	S_2	67	0.3750000	
30	0.0835616	K_2	68	0.3778538	
31	0.0848173	MSN_2	69	0.4138127	
32	0.0861872	$2SM_2$	70	0.4166666	
33	0.0869863		71	0.4195205	
34	0.0874429	$2S\upsilon 2$	72	0.4554794	
35	0.0876712	$2SN_2$	73	0.4583333	
36	0.0891552		74	0.4611872	
37	0.1178082	NO_3	75	0.4971461	
38	0.1194063	$2MS_3$			

fortnightly constituent (Msf), principal solar semidiurnal component (S_2), and variational constituent (μ_2) possess the predominant amplitudes in the data series projected onto the second mode.

In spite of the orthogonality of the principal components or the base vectors of the eigenspace, each of the PCs may be contaminated by the others (Ji 2011). This results in the presence of similar constituents in the frequency contents of various principal components. The commonly detected frequencies for eigenmodes 3 to 10 are given in Table 4. These modes contain signals on shorter temporal scales than the first two ones.

To come up with an idea about the efficiency of the KLE method in

Table 4. The commonly detected frequencies for eigenmodes three through ten.

No.	Freqency (hour^{-1})	symbol	No.	Freqency (hour^{-1})	symbol
1	0.0044520		48	0.2025114	MSO_5
2	0.0060502	Mqm	49	0.2026255	$2MS_5$
3	0.0071917	$2SMN$	50	0.2053652	MSP_5
4	0.0359589	σ_1	51	0.2084474	$2SK_5$
5	0.0374429	υK_1	52	0.2369863	$3MNK_6$
6	0.0431506		53	0.2372146	$3NKS_6$
7	0.0446347	$SO1$	54	0.2402968	$2M\upsilon 6$
8	0.0748858	$2NK_2S_2$	55	0.2428082	MSN_6
9	0.0763698	$2ML_2S_2$	56	0.2430365	$4MN_6$
10	0.0772831	$2MS_2K_2$	57	0.2441780	$2MSK_6$
11	0.0776255	μ_2	58	0.2442922	$2MT_6$
12	0.0788812	NA_2	59	0.2456621	$2SN_6$
13	0.0791095	NB_2	60	0.2457762	$2MSK_6$
14	0.0794520	$2KN_2S_2$	61	0.2470319	MST_6
15	0.0799086		62	0.3190639	$2MN_8$
16	0.0803652	α_2	63	0.3203196	$3MSNK_8$
17	0.0805936	KO_2	64	0.3205479	$3MN_8$
18	0.0825342		65	0.3207762	$3M\upsilon_8$
19	0.0832191	T_2	66	0.3220319	M_8
20	0.0834474	R_2	67	0.3222602	$4MKS_8$
21	0.0839041		68	0.3248858	$3MS_8$
22	0.0844748		69	0.3261415	$2SMN_8$
23	0.0853881	$2KMSN_2$	70	0.3263698	$2MSL_8$
24	0.0863013	$2MS_2N_2$	71	0.3275114	$2MST_8$
25	0.0871004		72	0.3276255	$2MS_8$
26	0.0889269	$3S_2M_2$	73	0.3279680	$2MSK_8$
27	0.0892694	$2SK_2M_2$	74	0.3289954	$3SN_8$
28	0.1192922	MO_3	75	0.3995433	$3M_2N_{10}$
29	0.1220319	SO_3	76	0.4010273	$4MN_{10}$
30	0.1251141	SK_3	77	0.4023972	$5MSK_{10}$
31	0.1279680	$2SO_3$	78	0.4038812	$3MSN_{10}$
32	0.1551369		79	0.4053652	$4MS_{10}$
33	0.1553652	$4M_2S_4$	80	0.4066210	$2MSN_{10}$
34	0.1566210	$2MNS_4$	81	0.4082191	$3M_2S_{10}$
35	0.1597031	$M\upsilon_4$	82	0.4097031	$2SMKN_{10}$
36	0.1607305	$2MSK_4$	83	0.4110730	$3S_2M_{10}$
37	0.1609589	MA_4	84	0.4813926	$5MSNK_{12}$
38	0.1611872	$2MRS_4$	85	0.4828767	$3M_2SN_{12}$
39	0.1613013	$2MKS_4$	86	0.4843607	$4MSN_{12}$
40	0.1636986	M_2SK_4	87	0.4857305	$5MT_{12}$
41	0.1639269	MR_4	88	0.4861872	$5MK_{12}$
42	0.1668949	SK_4	89	0.4872146	$3M_2SN_{12}$
43	0.1982876	$2MQ_5$	90	0.4874429	$6MSN_{12}$
44	0.1984018	$2NKMS_5$	91	0.4886986	$4M_2S_{12}$
45	0.1998858	$3MS_5$	92	0.4889269	$4MSK_{12}$
46	0.2012557	M_5	93	0.4915525	$3MS_{12}$
47	0.2013698	MB_5			

Table 5. The frequency content of tidal data as suggested by the application of LSHE technique (Mousavian and Hossainali, 2012).

No.	Frequency ($hour^{-1}$)	symbol
1	0.080489	M_2
2	0.083340	S_2
3	0.079020	N_2
4	0.083514	K_2
5	0.080775	MKS_2
6	0.080205	
7	0.080089	
8	0.083222	T_2
9	0.079201	υ_2
10	0.079980	
11	0.081004	
12	0.082034	L_2
13	0.038731	O_1
14	0.079872	
15	0.041771	K_1
16	0.161004	MN_4
17	0.078864	

reconstructing a periodic signal such as the tide, the constituents above are compared with those detected by the application of the LSHE method. Table 5 reports on the frequencies suggested by the latter technique. According to Table 5, constituents detected by least squares harmonic estimation is restricted to high frequency ones whereas both low and high frequency constituents have been efficiently identified here.

4. Conclusions

In this paper, the Karhunen-Loeve Expansion has been applied for investigating the tide as a non-linear system. For this purpose, an autoregressive process is used as the background noise model for the power spectra of each principal component. According to the obtained results, the first principal component includes most of the predominant frequencies inherent in the tidal data. While the higher order KLE modes mainly include the corresponding shallow water ones.

Moreover, the efficiency of this method is compared with the results of LSHE recently carried out for the identification of the tidal frequencies at the same station and using the same period of time. Similar to the LSHE method, frequency analysis using the applied technique is sensitive to the adopted background noise. Nevertheless, the comparison of the obtained results to those reported for the application of least squares harmonic estimation clearly proves the prominence of the applied method in this research.

From the total number of expected long period constituents (see appendix A) 73.3 percent have been successfully detected by the KLE whereas none of these frequencies are seen when least squares harmonic estimation is used. In the high frequency domain, including diurnal, semidiurnal and short periods, 44.3 percent of the total number of the expected constituents (which are partially listed in appendix B) have been identified in this research. The higher success rate in the detection of tidal frequencies obviously results in a more reliable reconstruction for the tidal time series when compared to the least squares harmonic estimation technique.

Appendix A

The List of long period constituents according to the standard list of tidal harmonic constituents published on the International Hydrographic Organization (IHO) website at http://www.iho.int/mtg_docs/com_wg/IHOTC/IHOTC_Misc/TWLWG_Constituent_list.pdf.

No.	Frequency ($hour^{-1}$)	symbol
1	0.0001140	Sa
2	0.0002281	Ssa
3	0.0003422	Sta
4	0.0013097	MSm
5	0.0015121	Mm
6	0.0028219	MSf
7	0.0030500	Mf
8	0.0041317	$S\upsilon_2$
9	0.0043340	SN
10	0.0043598	$MStm$
11	0.0045622	Mfm
12	0.0056438	$2SM$
13	0.0058720	$MSqm$
14	0.0060743	Mqm
15	0.0071560	$2SMN$

Appendix B

The List of diurnal, semidiurnal and short periods constituents according to the standard list of tidal harmonic constituents published on the International Hydrographic Organization (IHO) website (similar to Appendix A).

No.	Freqency ($hour^{-1}$)	symbol	No.	Freqency ($hour^{-1}$)	symbol
1	0.0357063	$2Q_1$	61	0.0846431	$MS\upsilon_2$
2	0.0359087	σ_1	62	0.0848454	MSN_2
3	0.0372185	Q_1	63	0.0850736	η_2
4	0.0374208	ρ_1	64	0.0853018	$2KMSN_2$
5	0.0387306	O_1	65	0.0861552	$2SM_2$
6	0.0388447	MS_1	66	0.0863576	$2MS_2N_2$
7	0.0389588	τ_1	67	0.0874650	$2S\upsilon_2$
8	0.0402428	M_1B	68	0.0876674	$2SN_2$
9	0.0402557	M_1	69	0.0878955	SKN_2
10	0.0402685	M_1A	70	0.0889772	$3S_2M_2$
11	0.0402685	M_1	71	0.0892053	$2SK_2M_2$
12	0.0404709	χ_1	72	0.1177299	MQ_3
13	0.0414385	π_1	73	0.1192420	MO_3
14	0.0415525	P_1	74	0.1192678	$2NKM_3$
15	0.0416666	S_1	75	0.1193561	$2MS_3$
16	0.0417807	K_1	76	0.1194702	$2MP_3$
17	0.0418948	ψ_1	77	0.1207671	M_3
18	0.0420089	ϕ_1	78	0.1207799	NK_3
19	0.0430905	θ_1	79	0.1220639	SO_3
20	0.0432928	MQ_1	80	0.1221780	MS_3
21	0.0443745	$2PO_1$	81	0.1222921	MK_3
22	0.0446026	SO_1	82	0.1222921	MK_3
23	0.0448308	OO_1	83	0.1236019	NSO_3
24	0.0463429	υ_1	84	0.1238043	$2MQ_3$
25	0.0733553	$2MN_2S_2$	85	0.1248859	$SP3$
26	0.0746393	$3MKS_2$	86	0.1250000	S_3
27	0.0746651	$2NS_2$	87	0.1251140	SK_3
28	0.0748675	$3MS_2$	88	0.1253422	K_3
29	0.0748933	$2NK_2S_2$	89	0.1279360	$2SO_3$
30	0.0759491	OQ_2	90	0.1553789	$4M_2S_4$
31	0.0761773	ε_2	91	0.1564605	$2MNK_4$
32	0.0763796	$M\upsilon 2S_2$	92	0.1566887	$2MNS_4$
33	0.0764054	MNK_2S_2	93	0.1568910	$2M\upsilon S_4$
34	0.0772331	$2MS_2K_2$	94	0.1579727	$3MK_4$
35	0.0774613	O_2	95	0.1579984	N_4
36	0.0774870	$2N_2$	96	0.1582008	$3MS_4$
37	0.0776894	μ_2	97	0.1592824	$MSNK_4$
38	0.0787710	SNK_2	98	0.1595106	MN_4
39	0.0788851	NA_2	99	0.1597130	$M\upsilon_4$
40	0.0789992	N_2	100	0.1597388	$MNKS_4$
41	0.0791133	NB_2	101	0.1607946	$2MSK_4$
42	0.0792016	υ_2	102	0.1609087	MA_4
43	0.0794555	$2KN_2S_2$	103	0.1610228	M_4
44	0.0802832	MSK_2	104	0.1611368	$2MRS_4$
45	0.0803090	γ_2	105	0.1612509	$2MKS_4$
46	0.0803973	α_2	106	0.1623325	SN_4
47	0.0805114	M_2	107	0.1625349	$3MN_4$
48	0.0806254	MSP_2	108	0.1625607	NK_4
49	0.0807395	δ_2	109	0.1636165	M_2SK_4
50	0.0809677	$2KM_2S_2$	110	0.1637306	MT_4
51	0.0815930	$2SNMK_2$	111	0.1638447	MS_4
52	0.0818211	λ_2	112	0.1639588	MR_4
53	0.0820235	L_2	113	0.1640728	MK_4
54	0.0820493	L_2B	114	0.1651545	$2SNM_4$
55	0.0820493	NKM_2	115	0.1653568	$2MSN_4$
56	0.0831051	$2SK_2$	116	0.1655850	$2MKN_4$
57	0.0832192	T_2	117	0.1665525	ST_4
58	0.0833333	S_2	118	0.1666666	S_4
59	0.0834474	R_2	119	0.1668948	SK_4
60	0.0835614	K_2	120	0.1671229	K_4

References

Allen M. R. and Smith L. A., 1996, Monte Carlo SSA: Detecting irregular oscillations in the presence of coloured noise, J. Clim., 9, 3373–3404.

Amiri-Simkooei A. R., 2007, Least-squares variance component estimation: Theory and GPS applications, Ph.D. thesis, Delft University of Technology, Publication on Geodesy, 64, Netherlands Geodetic Commission, Delft.

Brockwell P. J. and Davis R. A., 1991, Time series: Theory and Methods, Springer-Verlag, New York, ISBN: 0-387-97429-6.

Cartwright D. E. and Tayler R. J., 1971, New computations of the tide-generating potential, Geophys. J. Roy. Astron. Soc., 23, 45–74.

Dong D., Fang P., Bock Y., Webb F., Prawirodirdjo L., Kedar S. and Jamason P., 2006, Spatiotemporal filtering using principal component analysis and Karhunen-Loeve expansion approaches for regional GPS network analysis, J. Geophys. Res., no. 111, doi: 10.102.

Doodson A. T., 1921, The harmonic development of the tide generating potential, Proc. R. Soc. A, 100: 305–329.

Foreman, M. G. G., Cherniawsky J. Y. and Ballantyne V. A., 2009, Versatile Harmonic Tidal Analysis: Improvements and Applications, J. Atmos. Oceanic Technol., 26, 806–817.

Ghil M., Allen M. R., Dettinger M. D., Ide K., Kondrashov D., Mann M. E., Robertson A. W., Saunders A., Tian Y., Varadi F. and Yiou, P., 2002, Advanced spectral methods for climatic time series, Rev. Geophys., 40, 1003–1043.

Hartmann T. and Wenzel H. G., 1995, The HW95 tidal potential catalogue. Geophys. Res. Lett, 22, 3553–3556.

House M. R., 1995, Orbital forcing timescales: an introduction, Geological Society, London, Special Publications, 85, 1-18.

Ji, K. H., 2011, Transient signal detection using GPS position time series, Ph.D. thesis, 243 pp., Mass. Inst. of Technol., Cambridge, 20 July.

Jay D. A. and Flinchem E. P., 1997, Interaction of fluctuating river flow with a barotropic tide: A test of wavelet tidal analysis methods, J. Geophys. Res., 102, 5705–5720.

Kudryavtsev S. M., 2004, Improved harmonic development of the Earth tide-generating potential, J. Geod., 77, 829–838.

Longman I.M., 1959, Formulas for computing the tidal accelerations due to the Moon and the Sun, J. Geophys. R., 64: 2351–2355.

Mann M. E. and Lees J. M.. 1996, Robust Estimation of Background Noise and Signal Detection in Climatic Time Series, Clim.Change, 33, 409–445.

Mousavian R. and Mashhadi Hossainali M., 2012, Detection of main tidal frequencies using least squares harmonic estimation method, J Geod. Sci., 3, 224-233.

Munk W.H. and Cartwright D.E., 1966, Tidal spectroscopy and prediction. Phil. Trans. R. Soc. A, 259: 533–581.

Penland C. and Magorian T., 1993, Prediction of Niño 3 sea surface temperatures using linear inverse modeling, J. Clim., 6, 1067– 1076.

Preisendorfer R. W., 1988, Principle Component Analysis in Meteorology and Oceanography, Elsevier Sci., New York, ISBN: 0-444-41710-9.

Press, W. H., Flannery B. P., Teukolsky S. A. and Vettering W. T., 1992, Numerical Recipes in C, 2nd ed., Cambridge Univ. Press, New York, ISBN:0-521-43108-5.

Rundle, J. B., Klein W., Tiampo K. F., and Gross S., 2000, Linear pattern dynamics in nonlinear threshold systems, Phys. Rev. E, 61, 2418– 2432.

Roosbeek F., 1995, RATGP95: a harmonic development of the tide-generating potential using an analytical method, Geophys. J. Int., 126: 197–204.

Savage, J. C., 1988, Principal component analysis of geodetically measured deformation in Long Valley caldera, eastern California, 1983 – 1987, J. Geophys. Res., 93, 13,297–13,305.

Tamura Y., 1987, A harmonic development of the tide generating potential, Bulletin d'Information des Marées Terrestres 99: 6813–6855.

Tiampo K. F., Rundle J. B., Klein W., Ben-Zion Y. and McGinnis S., 2004, Using eigenpattern analysis to constrain seasonal signals in southern California, Pure Appl. Geophys., 1991–2003.

Torrence C. and Compo G. P., 1998, A Practical Guide toWavelet Analysis, B. Am. Meteorol. Soc., 79, 61–78.

Wahr J., 1995, Earth Tides, Global Earth Physics, A Handbook of Physical Constants, AGU Reference Shelf, 1, 40-46.